CHEMISTRY
A EUROPEAN JOURNAL

DOI: 10.1002/chem.200501352

The Prediction of the Nuclear Quadrupole Splitting of ^{119}Sn Mössbauer Spectroscopy Data by Scalar Relativistic DFT Calculations

Jesper W. Krogh,[a] Giampaolo Barone,*[b] and Roland Lindh*[c]

Abstract: The electric field gradient components for the tin nucleus of 34 tin compounds of experimentally known structures and ^{119}Sn Mössbauer spectroscopy parameters were computed at the scalar relativistic density functional theory level of approximation. The theoretical values of the electric field gradient components were used to determine a quantity, V, which is proportional to the nuclear quadrupole splitting parameter (ΔE). In a subsequent linear regression analysis the effective nuclear quadrupole moment, Q, was evaluated. The value of $(11.9 \pm 0.1)\,\mathrm{fm}^2$ is a significant improvement over the non-relativistic result of $(15.2 \pm 4.4)\,\mathrm{fm}^2$ and is in agreement with the experimental value of $(10.9 \pm 0.8)\,\mathrm{fm}^2$. The average mean square error $\Delta E_{\mathrm{calcd}} - \Delta E_{\mathrm{exptl}} = \pm 0.3\,\mathrm{mm\,s^{-1}}$ is a factor of two smaller than in the non-relativistic case. Thus, the approach has a quality which provides accurate support for the structure interpretation by ^{119}Sn spectroscopy. It was noted that geometry optimization at the relativistic level does not significantly increase the quality of the results compared with non-relativistic optimized structures. The accuracy in the approach called on us to consider the singlet–triplet state nature of the electronic structure of one of the investigated compounds.

Keywords: density functional calculations · Moessbauer spectroscopy · nuclear quadrupole splitting · tin

Introduction

It was recently reported[1] that non-relativistic density functional theory (DFT) calculations of the electric field gradient (EFG) at the tin nucleus can be used as a support of the structural interpretation of ^{119}Sn Mössbauer spectroscopy data.[2] In particular, by using an all-electron basis set, the EFG components, V_{xx}, V_{yy} and V_{zz}, at the tin nucleus were calculated for the fully optimized structures of 34 Sn^{II} and Sn^{IV} compounds, of known structure and ^{119}Sn Mössbauer parameters. These were used to determine the quantity V [Eq. (1)],

$$V = V_{zz}\left[1 \cdot \frac{1}{3}\frac{V_{xx}-V_{yy}}{V_{zz}}^2\right]^{1/2} \quad (1)$$

which is related to the quadrupole splitting (ΔE) parameter by Equation (2),

$$\Delta E = 1/2 \cdot eQ \cdot V \quad (2)$$

where e is the electronic charge and Q is the nuclear quadrupole moment of the tin nucleus.

The linear fitting of the correlation of the experimental ΔE values versus the corresponding calculated V values produced a correlation coefficient, R, equal to 0.982. Using the slope as a calibration constant, it was possible to obtain theoretical values of ΔE through the calculated values of V according to Equation (3).[1]

$$\Delta E_{\mathrm{calcd}} = 0.93V \pm 0.58\,\mathrm{mm\,s^{-1}} \quad (3)$$

This approach proved to be a useful tool for obtaining detailed structural information on tin and organotin deriva-

[a] J. W. Krogh
Department of Theoretical Chemistry, University of Lund
P.O.B 124, 221 00 Lund (Sweden)
[b] Dr. G. Barone
Dipartimento di Chimica Inorganica e Analitica
"Stanislao Cannizzaro", Università di Palermo
Viale delle Scienze, Parco d'Orleans II, 90128 Palermo (Italy)
Fax: (+39) 091-427-584
E-mail: gbarone@unipa.it
[c] Prof. R. Lindh
Department of Chemical Physics, Lund University
P.O.B 124, 221 00 Lund (Sweden)
Fax: (+46) 46-22-24119
E-mail: Roland.Lindh@chemphys.lu.se

tives, and represents a significant step forward compared to the point charge model, which is still well accepted for structure assignment but restricted to the determination of the coordination geometry of organotin(IV) compounds.[2] The suggested computational method is specifically useful for the structural analysis of tin compounds for which X-ray crystallography cannot be performed, for example when it is not possible to obtain suitable crystals.

The values that the ΔE parameter may assume are indeed strictly related to subtle changes in the core electron density of the tin atom, determined by the electronic properties of the ligands and by the coordination geometry of the metal complex. Hence, the disagreement between experimental and calculated parameters, could be attributed to 1) the geometrical differences between the structures calculated in vacuo and the experimentally considered solid-state structures, 2) the deficiencies of the basis set used to describe the inner region and accurately determine the EFG components, and 3) the neglect of relativistic effects. It has been shown that the deviations of ΔE_{calcd} from the linear trend do not depend on the observed discrepancies between the solid-state and the calculated structures.[1] The basis set deficiency, however, is an issue that needs consideration. Finally, the importance of relativistic effects in the evaluation of the hyperfine parameter ΔE for tin compounds remains up to now an open question. The effect of relativistic contributions on valence properties of tin compounds has recently been taken into account by the relativistic elimination of small components (RESC) method,[3] or by the two-component approach using the zero order regular approximation (ZORA).[4] The latter include both the spin-orbit interaction and the scalar relativistic terms. The relativistic DFT calculations gave good agreement with experiment, and within a few picometers in optimized geometries. Only small tin compounds, however, have been considered so far, for example, SnY_4 or SnY_3 (Y = H, CH_3, C_2H_5, F, Cl, Br, I, At).[3,4]

In the present study the issues of basis set and relativistic effects are addressed and the results of scalar relativistic DFT calculations on tin compounds containing up to 94 atoms, using the Douglas–Kroll–Hess[5] (DKH) approximation, are reported.

Results and Discussion

The ^{119}Sn Mössbauer parameters η, V_{zz} and V, obtained by the DFT calculations (see Computational Details), and the experimental ΔE values, are reported in Table 1. The correlation plots of the experimental ΔE versus the corresponding values of V obtained at the non- and relativistic DFT level for compounds **1**–**34** are shown in Figure 1. In compari-

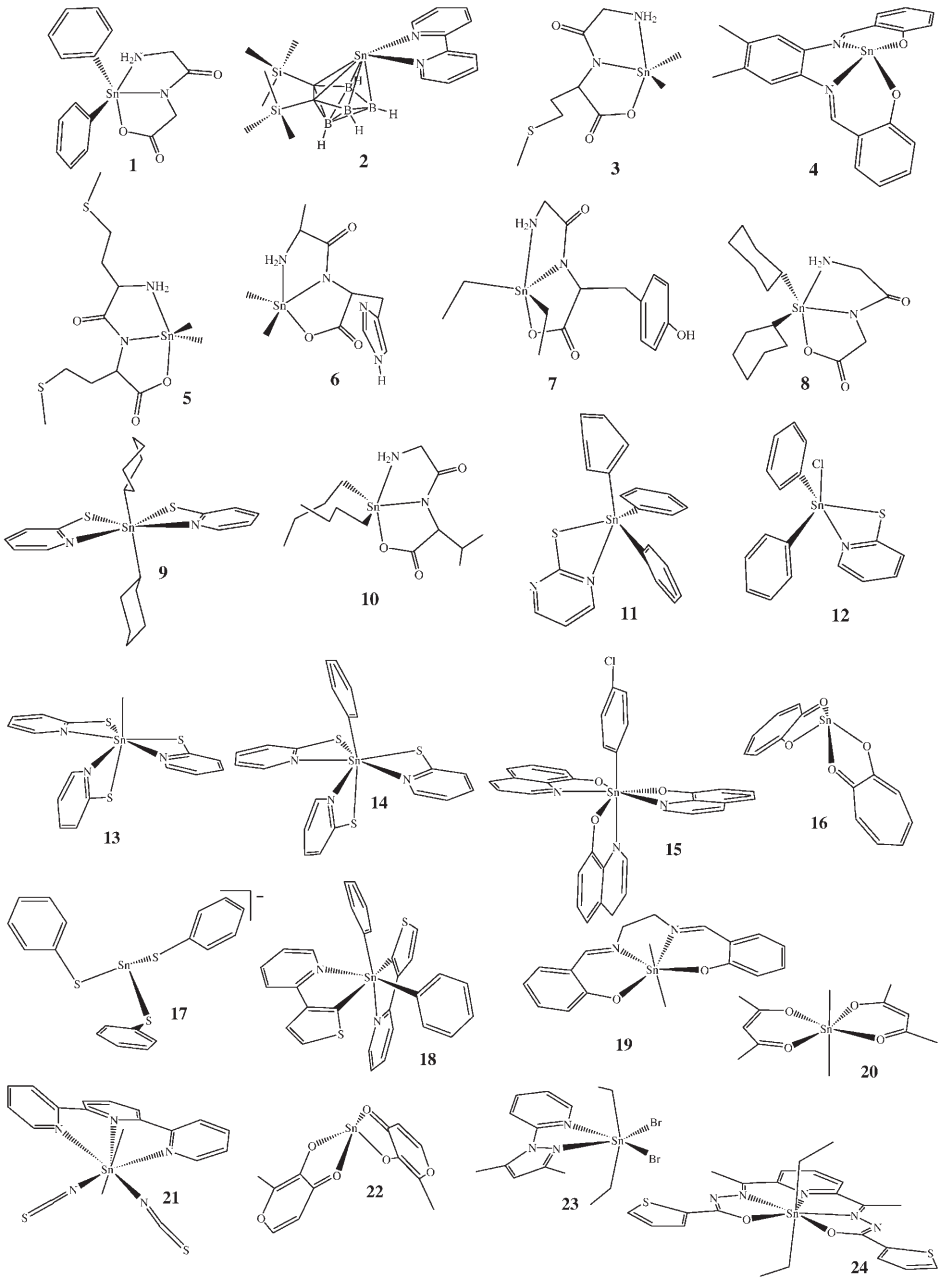

son with the non-relativistic DFT results[1] the data points are evidently less scattered. The results of the linear fitting over 33 points (compound **2** was excluded, see discussion below), by imposing the condition of zero intercept, produced a slope of $(0.73\pm0.01)\,\mathrm{mm\,s^{-1}\,au^{-1}}$, with a correlation coefficient $R=0.996$. This is to be compared with the non-relativistic DFT results of $R=0.982$ and a slope of $(0.93\pm0.03)\,\mathrm{mm\,s^{-1}\,au^{-1}}$.[1] Using the slope as a calibration constant, it is possible to obtain calculated values of ΔE (Table 1) from the corresponding values of V, by using Equation (4).

$$\Delta E_{\mathrm{calcd}} = (0.726 \cdot V \pm 0.27)\,\mathrm{mm\,s^{-1}} \quad (4)$$

Here the error bar represents the average mean square error for the 33 compounds. The estimated value of the nuclear quadrupole moment of tin is $Q=(11.9\pm0.1)\,\mathrm{fm^2}$, which is to be compared with the previous theoretical result, $Q=(15.2\pm4.4)\,\mathrm{fm^2}$,[1] and the experimental value, $|Q|=(10.9\pm0.8)\,\mathrm{fm^2}$.[6] Interestingly, the error bar in the present calculation is smaller than the experimental error. It could be argued that the increase of the correlation coefficient in the present study is mainly due to a better description of the core electrons of tin by the use of a tighter basis set (see Computational Details), while the scalar relativistic corrections mainly affect the slope of the correlation. It should be pointed out that to investigate these contributions separately would require the development of a non-relativistic basis similar in quality to the atomic natural orbital relativistic core-correlated (ANO-RCC) basis sets.[7]

For compounds **5**, **7**, **10**, and **12** a change in the sign of V was noted at the relativistic level, as compared to what was previously obtained (see Table 1).[1] It has been reported that when the asymmetry parameter, η, is roughly greater than 0.7 it is difficult to experimentally determine the sign of V_{zz} (and ΔE), by Mössbauer–Zeeman measurements.[8] In this respect it was interesting to observe that, for the above-mentioned compounds, the non-relativistic η values were greater than 0.95. That is, the values of the components V_{yy} and V_{zz} were almost equal but with opposite sign. However, in the present work the η values of compounds **5**, **7**, and **10** decreased to less than 0.72. Accordingly, the sign, of the corresponding experimental ΔE values were changed. For compound **12**, on the other hand, the current value of η is close to 1 (within the third significant digit). Hence it should not be possible to experimentally determine the sign of V_{zz}. Considering that it does not change the quality of the fit, a positive sign was assigned to the computed V value of compound **12**.

It must be pointed out that the EFG components have been computed by non-relativistic property integrals. The neglect of the so-called picture-change effect in the computation of the EFG has been analyzed by Kellö and Sadlej.[9] The error of this neglect is systematic and has been demonstrated to give an overestimate of 8% for the EFG of iodine. A similar sized overestimate is expected in the current investigation, and indeed the computed Q value is about 9% higher than the experimental finding.[6] This error is acceptable considering the accuracy of the DFT method and that theoretical gas-phase results are compared with experimental solid-state results. Moreover, the systematic error associated with V should be cancelled in $\Delta E_{\mathrm{calcd}}$, since it is determined through a calibration with the experimental values of ΔE. Hence, according to Equation (4), the calculated nuclear quadrupole splitting of ^{119}Sn is expected to be within $\pm0.3\,\mathrm{mm\,s^{-1}}$ of the experimental value.

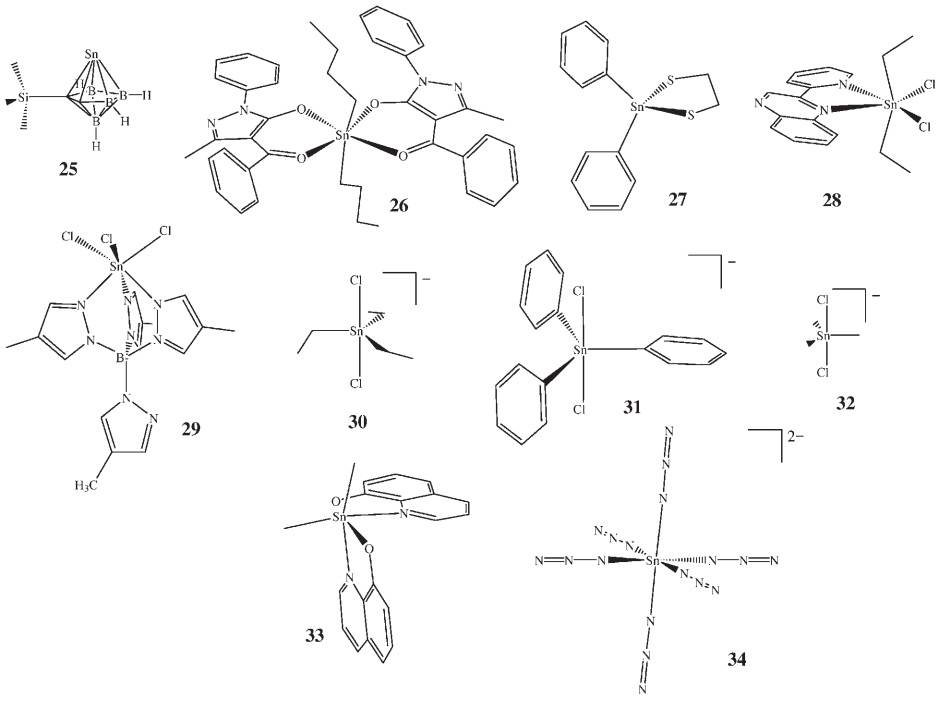

During the processing of the data the error of compound **2**[10] (see Figure 2) was noted to be larger than that observed of the other molecules (see the triangle symbol on the right side of the line in Figure 1). This discrepancy could be argued to be associated with the electronic structure of **2**. In particular, it is possible that due to the presence of the 2,2′-bipyridine ligand the ground state of **2** could have a component of triplet state configuration. In fact, Sn^{II} complexes are known to have low-energy singlet–triplet state electronic transitions (n–p transitions), often occurring in the visible range, depending on the electronic and steric properties of the ligands.[11] Moreover, the 2,2′-bipyridine ligand, can

Table 1. ^{119}Sn Mössbauer parameters obtained from relativistic DFT calculations for the compounds considered.

Compound[a]	η[b]	V_{zz}[b]	V[c]	ΔE[d]	ΔE_{calcd}[e]	ΔE_{calcd}[f]
1	0.62	−3.19	−3.38	−2.24	−2.46	−2.14
2 singlet	0.54	5.21	5.46	(+)2.73	3.96	4.12
2 triplet	0.68	1.97	2.11		1.53	1.93
3	0.64	−3.33	−3.55	(−)2.53	−2.57	−2.68
4	0.52	2.18	2.28	(+)1.34	1.65	2.31
5	0.67	−3.30	−3.54	(−)2.94	−2.57	2.68
6	0.58	−3.35	−3.54	(−)3.20	−2.57	−2.67
7	0.71	−3.54	−3.83	(−)2.87	−2.78	2.87
8	0.70	−3.57	−3.85	(−)3.11	−2.80	−2.63
9	0.61	3.70	3.92	(+)2.84	2.85	2.15
10	0.72	−3.47	−3.76	(−)2.65	−2.73	2.70
11	0.19	−2.19	−2.20	(−)1.65	−1.60	−0.83
12	1.00	3.16	3.65	(+)2.58	2.65	−2.01
13	0.09	3.03	3.04	(+)2.23	2.20	2.02
14	0.17	2.94	2.95	(+)1.89	2.14	1.58
15	0.07	2.40	2.40	(+)1.71	1.74	1.57
16	0.61	2.69	2.86	(+)1.98	2.07	2.32
16[g]	0.61	2.74	2.90			
17	0.00	1.84	1.84	(+)1.38	1.33	1.53
18	0.31	−1.34	−1.36	(−)0.73	−0.99	−0.85
19	0.13	5.28	5.29	(+)3.46	3.84	4.07
20	0.11	5.68	5.69	(+)3.93	4.13	4.27
21	0.27	5.26	5.32	(+)4.29	3.86	4.14
22	0.62	2.90	3.08	(+)1.99	2.24	2.35
22[g]	0.64	2.98	3.17			
23	0.09	5.13	5.14	(+)4.00	3.73	3.31
24	0.14	5.42	5.44	(+)3.72	3.94	4.12
25	0.65	4.50	4.80	(+)2.79	3.48	3.48
25[g]	0.64	4.50	4.80			
26	0.07	5.86	5.87	(+)4.14	4.26	4.30
27	0.61	−2.15	−2.28	(−)1.56	−1.65	−0.87
28	0.05	5.16	5.16	(+)3.98	3.75	3.24
29	0.18	−0.11	−0.11	(−)0.43	−0.08	−0.36
30	0.00	−4.38	−4.38	−3.49	−3.18	−2.59
30[g]	0.01	−4.53	−4.53			
31	0.00	−4.00	−4.00	−3.02	−2.90	−1.89
32	0.00	−4.14	−4.14	−3.31	−3.01	−2.43
32[g]	0.00	−4.34	−4.34			
33	0.48	2.91	3.02	+2.06	2.19	2.60
34	–	0.00	0.00	0.00	0.00	0.00
34[g]	–	0.00	0.00			

[a] The structures of compounds **1–34** are reported in reference [1]. [b] $\eta=(V_{xx}-V_{yy})/V_{zz}$ with $|V_{zz}|\geq|V_{yy}|\geq|V_{xx}|$. [c] $V=V_{zz}\cdot(1+1/3\cdot\eta^2)^{1/2}$, in atomic units. [d] Experimental values of the nuclear quadrupole splitting parameter (in mm s^{-1}), obtained from the literature (see reference [1]); the sign in brackets is added to ΔE following the sign of V obtained from theoretical calculations. [e] ΔE_{calcd} is the quadrupole splitting parameter calculated through the slope obtained by the linear fitting of Figure 1, according to Equation (4). [f] Quadrupole splitting parameter calculated at non-relativistic level,[1] through Equation (3). [g] Values of the ^{119}Sn Mössbauer parameters calculated after geometry optimization at the DKH relativistic level.

be considered a radical anionic ligand,[12] in which unpaired electrons are delocalized in the ligand π^* orbitals. Furthermore, it is known that main group metal complexes of 2,2′-bipyridine often have a triplet spin state in the ground or a low-lying excited state.[12] To investigate this the ^{119}Sn Mössbauer parameters η, V_{zz} and V were evaluated for the triplet state of **2** after optimizing its geometry at the non-relativistic level (see Table 1). In Figure 1, an arrow shows the shift of the V value when going from the singlet to the triplet state. The geometrical parameters of the tin environment of **2**, optimized in the singlet and in the triplet state, are reported in Table 2 and compared with the experimental data. It can be seen that there is a better agreement between the experimental values of the bond lengths and angles with those of the singlet state. In particular, it is noted that the values of the two Sn–N and the Sn–B4 distances (see Figure 2) are shorter in the triplet state, while the other Sn–C and Sn–B distances are longer. This result is indicative of a stronger interaction in the triplet state of the tin atom with bipyridine followed by a weaker interaction with the five-membered carborane ring. Considering the tight linear trend of the plot of Figure 1, we have to conclude that neither the singlet nor the triplet state produce a satisfactory fit with experimental data. However, some triplet state component in the singlet ground state wave function would reduce the deviation. This example shows that, by including scalar relativistic effects in the calculation of tin EFGs, it is possible to obtain better information about the electron configuration of the tin compounds investigated by ^{119}Sn Mössbauer spectroscopy. However, the ultimate tool to investigate compounds like **2** will require inclusion of spin-orbit effects.

For the six smallest compounds (**16**,[13] **22**,[13] **25**,[10] **30**,[14] **32**,[15] and **34**[16]) the effect of geometry optimization (see Table 3) on the computed EFG was investigated (see Table 1). The largest differences of about 5 and 3%, were observed for compounds **32** and **30**, respectively. For the other compounds no significant difference was observed. The results indicate that the relativistic approach slightly improves the agreement with the experimental structures for both bond lengths and angles. It was also noted that the correlation of V with the experimental ΔE slightly improved. It should be pointed out that the geometry optimization at the non-relativistic level already furnishes a satisfying result for the structural agreement with the experimental results,[1] and an excellent result for the evaluation of the ΔE_{calcd} parameter at DKH level, thus pro-

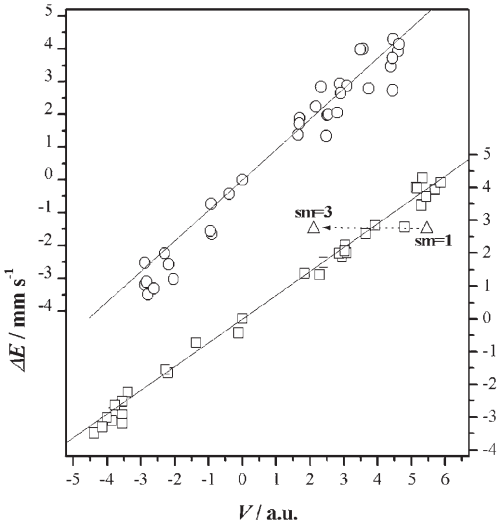

Figure 1. Correlation plot of the experimental ΔE values versus the corresponding calculated values of V, at the scalar relativistic (squares and ordinate to the right) and non-relativistic (circles and the ordinate to the left) DFT level, for compounds **1**–**34** (see Table 1). Triangle symbols are relative to the singlet (sm = 1) and triplet (sm = 3) states of compound **2**. The solid lines are the least-squares linear fits.

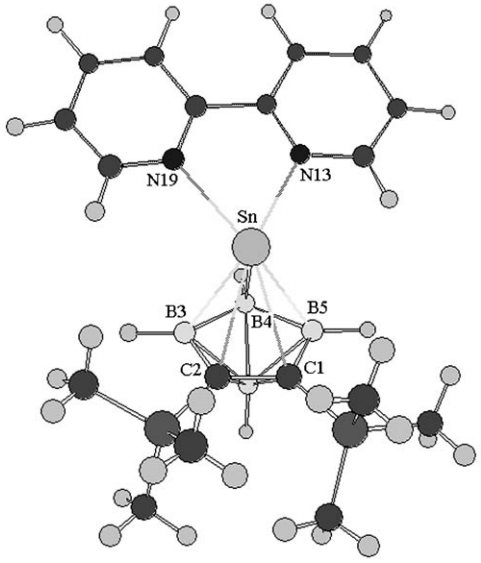

Figure 2. The structure of compound **2**. Element labels are as in reference [10].

viding effective support for the structural interpretation of ^{119}Sn Mössbauer spectroscopic data. Further improvement beyond this by reoptimizing the geometry at the relativistic level would be marginal and require considerable computational resources. It is our opinion that improvements first should address the neglect of the picture-change effect,[9] include spin-orbit effects, and consider the structural differences due to solid-state packing effects in the experimental structures.

For the six compounds discussed above the basis set saturation with respect to the EFG was investigated as well. The results showed only a deviation on the sixth to seventh significant digit of the computed EFG values.

Table 2. Relevant geometrical parameters (distances in Å and angles in degrees) of the tin environment of compound **2** (Figure 2), obtained by geometry optimization at non-relativistic DFT level (see text) of the singlet and triplet spin states (sm = 1 and sm = 3, respectively), compared to the corresponding experimental data (Exp).[10]

	sm = 1	sm = 3	Exp
Sn–C1	2.82	2.97	2.75
Sn–C2	2.79	2.93	2.70
Sn–B3	2.49	2.51	2.44
Sn–B4	2.38	2.31	2.37
Sn–B5	2.51	2.54	2.52
Sn–N13	2.62	2.24	2.49
Sn–N19	2.64	2.28	2.54
C1-Sn-N13	124.8	140.2	125.4
C1-Sn-N19	144.5	146.2	147.1
C2-Sn-N13	144.1	156.4	145.3
C2-Sn-N19	121.3	118.6	121.7
B3-Sn-N13	120.5	129.1	120.2
B3-Sn-N19	89.3	102.5	90.7
B4-Sn-N13	84.6	97.3	85.4
B4-Sn-N19	88.4	123.5	91.8
B5-Sn-N13	91.7	108.8	91.5
B5-Sn-N19	126.4	165.2	129.4
N13-Sn-N19	61.3	72.8	64.0
C1-Sn-C2	30.5	29.1	30.7
C1-Sn-B5	33.8	31.9	35.0
C2-Sn-B3	34.1	32.4	34.9
B3-Sn-B4	41.0	42.0	39.7
B4-Sn-B5	40.8	42.0	40.2

Conclusion

In a comparison between the non- and relativistic DFT models on 34 tin compounds a significantly improved agreement between the experimental and theoretical values of the ^{119}Sn Mössbauer nuclear quadrupole splitting was obtained by the inclusion of scalar relativistic effects. The relativistic corrections influenced the slope of the correlation plot, giving a value of the nuclear quadrupole moment of tin of about 9% larger than the experimental value. This deviation was expected, since the so-called picture-change effect was not considered. The use of the relativistic all-electron basis set increased the correlation coefficient of the fit. It was demonstrated that the results were stable with respect to further basis set improvements. Together, the basis set improvements and the inclusion of scalar relativistic effects enabled quantitative predictions of the ^{119}Sn Mössbauer nuclear quadrupole splitting parameter. Detailed information not accessible at non-relativistic level can thus be obtained on the electronic structure of tin compounds. In particular, the new approach led to a more detailed study of compound **2** with respect to the spin multiplicity of this species. Further improvement beyond what has been presented here will have to include corrections for the so-called picture-change effect, spin-orbit interactions, and solid-state packing effects in the calculated structures.

Table 3. Relevant geometrical parameters (distances in Å and angles in degrees) of the tin environment of the indicated compounds, calculated after geometry optimization at non-relativistic (NR) and at the relativistic (DKH) DFT level (see text) , compared to the corresponding experimental data (Exp).

Compound[a]	Parameter[a]	NR	DKH	Exp
16[13]	Sn−O1	2.211	2.191	2.140
	Sn−O2	2.296	2.293	2.258
	Sn−O3	2.296	2.293	2.242
	Sn−O4	2.211	2.191	2.14
	O1-Sn-O2	70.7	70.9	72.5
	O1-Sn-O3	79.3	80.2	77.1
	O1-Sn-O4	95.9	96.6	94.2
	O2-Sn-O3	134.7	136.1	137.4
	O2-Sn-O4	79.3	80.2	81.1
	O3-Sn-O4	70.7	70.9	72.0
22[13]	Sn−O1	2.376	2.370	2.324
	Sn−O2	2.178	2.156	2.129
	O2-Sn-O2′	93.5	93.9	94.5
	O1-Sn-O2′	80.2	80.9	81.4
	O1-Sn-O2	72.9	73.1	74.8
	O1-Sn-O1′	140.4	141.6	144.6
25[10]	Sn−C1	2.521	2.510	2.518
	Sn−C2	2.494	2.483	2.475
	Sn−B3	2.454	2.448	2.432
	Sn−B4	2.408	2.404	2.397
	Sn−B5	2.447	2.441	2.431
	C1-Sn-C2	34.3	34.4	34.7
	C1-Sn-B5	37.0	37.1	35.3
	C2-Sn-B3	36.9	37.0	37.9
	B3-Sn-B4	41.3	41.3	39.9
	B4-Sn-B5	41.4	41.4	39.8
30[14]	Sn−Claver	2.679	2.678	–[b]
	Sn−C	2.197	2.185	–
	C-Sn-C	120.0	120.0	–
	Cl-Sn-Cl	180.0	180.0	–
	C-Sn-Cl	90.0	90.0	–
32[14,15]	Sn−Claver	2.667	2.670	2.744
	Sn−C	2.183	2.166	2.121
	C-Sn-C	120.0	120.0	118.5
	Cl-Sn-Cl	180.0	180.0	179.2
	C-Sn-Cl	90.0	90.0	90.0
34[15,16]	Sn−Naver	2.113	2.091	2.15
	N1-Sn-N2	90.0	90.0	90.0
	N1-Sn-N3	180.0	180.0	180.0

[a] The structures of the compounds are reported in reference [1]. The element labels are as in the literature references. [b] Detailed experimental data of compound **30** were not given.

Computational Details

The EFGs for compounds **1**–**34** (excluding the so-called picture-change effect) were computed at the scalar relativistic DFT level of approximation in combination with the B3LYP[17] functional, the second-order Douglas–Kroll–Hess[5] (DKH) Hamiltonian, and an ANO-RCC[7] basis set. The basis set for tin was contracted to 6s5p3d1f; for all other atoms a contraction level of VDZP was used. The structures of the compounds were the fully optimized geometries at the non-relativistic B3LYP/DZVP level as reported by Barone et al.[1]

The eigenvalues of the diagonalized EFG components, V_{ii}, were used to derive the quantity V that is related to the theoretical ΔE value (see Equations (1) and (2)).

Geometry optimization was performed for the six smallest compounds **16**, **22**, **25**, **30**, **32**, and **34** (see Table 3). For this set of molecules a bigger basis was tested as well: 7s6p4d2f1g on Sn and VTZP for the remaining atoms. For the calculation with the larger basis set the two-electron integrals were approximated by the so-called Cholesky decomposition.[18] All calculations were carried out with the MOLCAS-6.3[19] software package.

The possibility to include the so-called picture-change effect according to the numerical differentiation approach suggested by Kellö and Sadlej was investigated.[9] After much disappointing work we found that numerical acceptable accuracy as a function of the parameters of the numerical differentiation had to be established molecule-by-molecule. We conclude that an analytical implementation of the picture-change effect of integrals for the computation of the expectation value of large molecular systems is the only efficient and reasonable approach.

Acknowledgements

This work has been supported by the Swedish Science Research Council (VR) and the Swedish Foundation for Strategic Research (SSF). The LUNARC computer center of Lund University and SNAC are acknowledged for generous allotment of computer resources.

[1] G. Barone, A. Silvestri, G. Ruisi, G. La Manna, *Chem. Eur. J.* **2005**, *11*, 6185–6191, and references therein.
[2] R. Barbieri, F. Huber, L. Pellerito, G. Ruisi, A. Silvestri in *Chemistry of Tin* (Ed.: P. J. Smith), Blackie, London, **1998**, ch. 14, pp. 496–540, and references therein.
[3] W. Lie, D. G. Fedorov, K. Hirao, *J. Phys. Chem. A* **2002**, *106*, 7057–7061.
[4] K. T. Giju, F. De Proft, P. Geerlings, *J. Phys. Chem. A* **2005**, *109*, 2925–2936.
[5] a) N. Douglas, N. M. Kroll, *Ann. Phys.* **1974**, *82*, 89–155; b) B. A. Hess, *Phys. Rev. A* **1986**, *33*, 3742–3748.
[6] H. Haas, M. Menningen, H. Andreasen, S. Damgaard, H. Grann, F. T. Pedersen, J. W. Petersen, G. Weyer, *Hyperfine Interact.* **1983**, 15/16, 215–218.
[7] a) B. O. Roos, R. Lindh, P.-Å. Malmqvist, V. Veryazov, P.-O. Widmark, *J. Phys. Chem. A* **2004**, *108*, 2851–2858; b) B. O. Roos, R. Lindh, P.-Å. Malmqvist, V. Veryazov, P.-O. Widmark, *J. Phys. Chem. A* **2005**, *109*, 6575–6579.
[8] A. Maddock, *Mössbauer Spectroscopy, Principles and Applications*, Horwood, **1997**, p. 65–67.
[9] V. Kellö, A. J. Sadlej, *Int. J. Quantum Chem.* **1998**, *68*, 159–174.
[10] N. S. Hosmane, P. de Meester, N. N. Maldar, S. B. Potts, S. S. C. Chu, R. H. Herber, *Organometallics* **1986**, *5*, 772–778.
[11] See for example: B. E. Eichler, A. D. Phillips, S. T. Haubrich, B. V. Mork, P. P. Power, *Organometallics* **2002**, *21*, 5622–5627.
[12] See for example: F. A. Cotton, G. Wilkinson, *Advanced Inorganic Chemistry*, Third Edition, Interscience, **1972**, p. 723.
[13] M. C. Barret, M. F. Mahon, K. C. Molloy, J. W. Steed, P. Wright, *Inorg. Chem.* **2001**, *40*, 4384–4388.
[14] R. V. Parish, C. E. Johnson, *J. Chem. Soc. A* **1971**, 1906–1910.
[15] S. Weng Ng, *Acta Crystallogr. Sect. C* **1995**, *51*, 1124–1125.
[16] S. E. Johnson, K. Pohlborn, H. Nöth, *Inorg. Chem.* **1991**, *30*, 1410–1412.
[17] A. D. Becke, *J. Chem. Phys.* **1993**, *98*, 5648 –5652.
[18] a) H. Koch, A. Sanchez de Meras, T. B. Pedersen, *J. Chem. Phys.* **2003**, *118*, 9481–9484; b) F. Aquilante, G. Ghigo, T. B. Pedersen, A. Sancez de Meras, H. Koch, unpublished results.
[19] a) V. Veryazov, P.-O. Widmark, K. Serrano-Andrés, R. Lindh, B. O. Roos, *Int. J. Quantum Chem.* **2004**, *100*, 626–635; b) G. Karlström, R. Lindh, P.-Å. Malmqvist, B. O. Roos, U. Ryde, V. Veryazov, P.-O. Widmark, M. Cossi, B. Schimmelpfennig, P. Neogrady, L. Seijo, *Comput. Mater. Sci.* **2003**, *28*, 222–239.

Received: October 31, 2005
Revised: January 31, 2006
Published online: May 2, 2006

